Front. Phys. China, 2009, 4(3): 297–306
DOI 10.1007/s11467-009-0021-y

REVIEW ARTICLE

Studies on structural defects in carbon nanotubes

Hai-yan HE (何海燕), **Bi-cai PAN** (潘必才)(✉)

Hefei National Laboratory for Physical Sciences at the Microscale, Department of Physics, University of Science and Technology of China, Hefei 230026, China

E-mail: bcpan@ustc.edu.cn

Received February 3, 2009; accepted February 15, 2009

Structural defects in carbon nanotubes (CNTs) have been paid much attention, because they influence the properties of the CNTs to some extent. Among various defects in CNTs, both single vacancies and Stone–Wales (SW) defects are the simple and common ones. In this paper, we review the progress of research in these two kinds of defects in CNTs. For single vacancies, we first address their different structural features in both zigzag and armchair CNTs, and their stabilities in CNTs with different sizes and different symmetries systematically. The presence of the single vacancies in CNTs not only influences the electronic structures of the systems, but also affects the vibrational properties of the tubes. Nevertheless, being active chemically, the single vacancies in the tubes prefer to interact with adsorbates nearby, of which the interaction of the defects with hydrogen atom, hydrogen molecule and some small hydrocarbon radicals (–CH, $–CH_2$ and $–CH_3$) are discussed. The former is associated with H storage and the latter is of merit to improve the local structure of the defect in a CNT. For the Stone–Wales defect, we mainly focus on its stability in various CNTs. The influence of the SW defects on the conductance of CNTs and the identification of such a defect in CNT is described in brief.

Keywords nanotubes, defects, adsorption, theoretical calculation

PACS numbers 31.15.es, 61.72.J-, 61.46.Fg

Contents

1 Introduction

Carbon nanotubes (CNTs) have aroused great interests in the areas of nano-science and nano-devices, since they were discovered [1]. This is due to that carbon nanotubes not only have unique anisotropic structures but also have various novel properties, involving unique mechanical, electrical, chemical and vibrational properties [2–11] . However, a realistic carbon nanotube is not defect-free, and it unavoidably contains many kinds of structural defects, which can be generated during the growth [12] or under electron irradiation [13, 14]. Undoubtedly, the existence of defects in CNTs should influence the physical and chemical properties of the CNTs to some extent. Therefore, studying the structural defects in CNTs is one of the fundamental issues for its potential applications.

The common structural defects existing in CNTs are atomic vacancies and topologic defects, of which the former corresponds to the deficiency of carbon atoms in a CNT, and the latter is associated with the network topology deviated from the hexagon rings. These defects have been studied extensively both theoretically and experimentally [15–27]. Experiments observe that carbon nanotubes can be released under electrons or ions irradiation [16, 22], leaving behind vacancies in CNTs. Once vacancies occur in CNTs, the dangling bonds at the vacancies may serve as bridges for the chemical connection between CNTs [23] or as active sites for adsorbates. Topological defects are usually observed in the bend junctions [28] and tip images [29] of CNTs, which significantly influences the electronic, mechanical, and transport properties of CNTs [30–34]. For example, Vi-

cent *et al.* [32] reported that both the band gap widths and the density of states at Fermi level of the CNTs were changed by the topological defects. Cohen *et al.* [33] found that the pentagon-heptagon pair defects produced quasibound states, through studying the conductance of metallic carbon nanotubes with the defects.

Among various vacancies, a single vacancy is the simplest one. An ideal single vacancy is formed by removing a carbon atom from the wall of a carbon nanotube, leaving three dangling bonds behind in the local structure. Meanwhile, a Stone–Wales (SW) defect is a commonly observed topologic defect in CNTs, which consists of two pentagons and two heptagons. Comparably, single vacancies are much more chemically active than SW defects. With dangling bonds, a single vacancy easily interacts with many kinds of adsorbates, such as molecules, radicals and metals. In contrast, SW defects are much more stable.

This paper reviews the main progress in single vacancies and SW defects in CNTs, including the structural features, formation energies and stabilities of these defects in different types of carbon nanotubes. Moreover, the influence of the defects on the properties of the carbon nanotubes is discussed. In addition, the interaction of a single vacancy with a hydrogen atom, hydrogen molecule or a small hydrocarbon radical (–CH, $–CH_2$ or $–CH_3$) is described in detail.

2 A single atomic vacancy

2.1 Structural patterns and stability of a single vacancy

As mentioned above, an ideal single vacancy in either armchair or zigzag carbon nanotube [Fig. 1 (a) and (c)] is chemically active. After full relaxation, the ideal single vacancy in a (n, n) carbon nanotube converts to a so-called 5-1DB defect consisting of a pentagon and an atom with a dangling bond (DB), with C3 bonding to either C1 or C2 [Fig. 1 (a)]. The defect pattern is shown in Fig. 1 (b). While in the case of a zigzag tube $(n, 0)$, the ideal vacancy [Fig. 1 (c)] may transform to be 5-1DB-T [Fig. 1 (d)], in which the orientation of the new bond of either C1–C3 or C2–C3 tilts against the tube axis, or 5-1DB-P [Fig. 1 (e)], in which the formed new bond of C1–C2 is perpendicular to the tube axis. These two kinds of configurations for a single vacancy in a $(n, 0)$ tube are stable after optimization.

Different structural patterns of 5-1DB, 5-1DB-P and 5-1DB-T have different stabilities. Figure 2 plots the formation energies of 5-1DB, 5-1DB-P and 5-1DB-T as a function of the radii of CNTs, together with the formation energy of a single vacancy in graphite. It is clearly

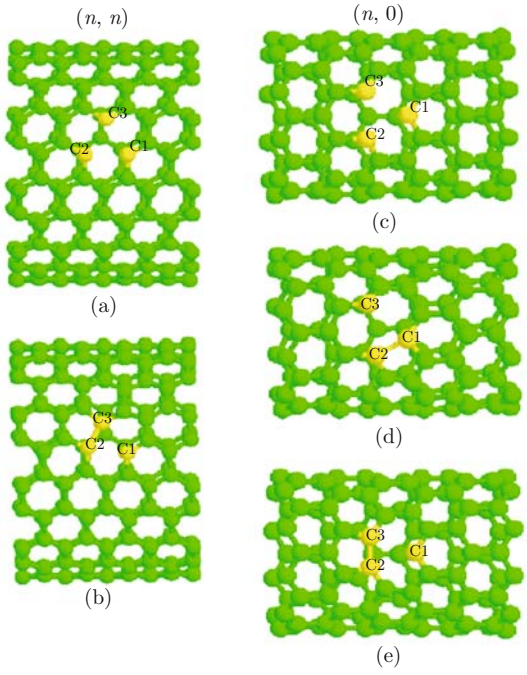

Fig. 1 Configurations of ideal vacancies in **(a)** (n, n) tubes and **(b)** $(n, 0)$ tubes. Carbon atoms in the vicinity of the defect are labeled as C1, C2 and C3, with light color.

shown that the defect formation energies in the defected $(n, 0)$ and (n, n) CNTs with nearly the same radius follow the order of E(5-1DB-T)> E(5-1DB)> E(5-1DB-P) except for some smaller tubes. Among these three kinds of defects, the 5-1DB-P defect is the most energetically preferable. On the other hand, for (n, n) tubes, the formation energies of 5-1DB defects increase monotonically with increasing tube radius. In contrast, for $(n, 0)$ tubes, the formation energies of 5-1DB-P and 5-1DB-T follow steplike and sawtoothlike trends, respectively. The formation energies of the defected $(n, 0)$ tubes with n=3m (m=2−5) are a little lower than those of their neighbors,

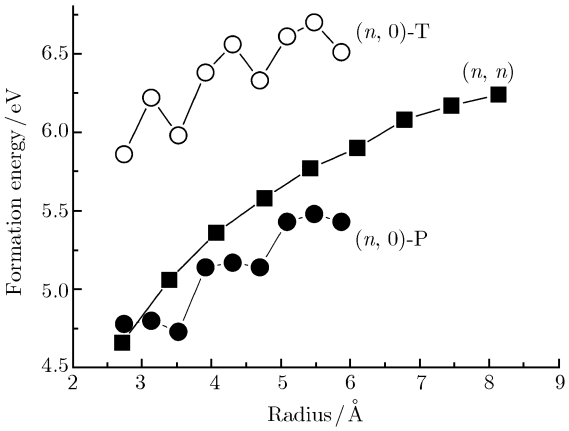

Fig. 2 Defect formation energy as a function of radius of a carbon nanotube. Down-triangles stand for 5-1DB defects in (n, n) tubes, filled squares for 5-1DB-P defects in $(n, 0)$ tubes, and open squares for 5-1DB-T defects in $(n, 0)$ tubes. Reprinted with permission from Ref. [17].

(n−1, 0) and (n+1, 0) tubes. This character is similar to the periodic features which are found in the evolution of energy gaps in perfect (n, 0) tubes [35]. Essentially, such observed periodic features are associated with the intrinsic geometrical property of the related perfect (n, 0) tubes.

2.2 Influence of single vacancies in properties of CNTs

Studies [17, 36] have revealed that the structural distortion caused by a single vacancy in a tube is localized spatially within two atomic shells. Therefore, when the point defects in CNTs are dilute, the σ-like hybridization in a whole system is not altered significantly. However, the presence of a single vacancy in a CNT destroys the original local σ-like hybridization around the vacancy by breaking the local symmetric structure of a perfect carbon nanotube, and thus introducing some new features in the properties of the CNT.

As for electronic properties, a perfect carbon nanotube is either metallic or semiconducting, depending on the chirality of the tube. When a single vacancy presents in a CNT, the conductive property of the system is not changed, but its electronic structure is modified. The electronic states induced by the single vacancies in the tubes are localized. Typically, for an armchair carbon nanotube of (8, 8), the presence of single vacancies does not alter the metallic conductivity of the system, but induces some typical states at about 0.2 eV above the Fermi level. These states predominately result from the atoms in two shells around the single vacancy. On the other hand, when a single vacancy is introduced to (14, 0) CNT, the defect states also appear at about 0.2 eV above the Fermi level. In addition, for a 5-1DB defect in (8, 8) tube, the 2s, $2p_x$, $2p_y$ and $2p_z$ orbitals of the DB atom heavily hybridize each other, where z axis is along the tube axis. In contrast, for the 5-1DB-T (5-1DB-P) defect in (14, 0) tube, the components of $2p_y$ ($2p_z$) of the defect states are much larger than those from the other three atomic orbitals of the DB atom. This implies that the hybridization of the atomic orbitals of the DB atoms is strongly dependent on the chirality of the tube.

Vibration is an intrinsic property of a system, which is tightly coupled with the geometry of the system. For a given carbon nanotube containing individual vacancies, the atomic structure around the defect is quite different from that of the perfect portion. Such a structural change affects the vibrational property of the tube. For carbon nanotubes of (n, 0) (n=7−9) with 5-1DB-P defects, the first-principle calculations at the level of local density approximation [37–39] combined with the frozen phonon method [40] have been performed to study the phonon spectra [36]. The calculations show that if the density of the single vacancies in a CNT is very small, the perturbation arising from the single vacancy to the lattice dynamics of the tube is localized. Similar to the case of the radial breathing mode (RBM) existing in vibrational spectra of each carbon nanotube, an RBM-like mode, in which the displacements of the carbon atoms are all in radial direction with different amplitudes, is found in vibrational modes of the carbon nanotubes containing single vacancies. Moreover, the comparison of the vibrational density of states (VDOS) between CNTs containing 5-1DB defects and the corresponding perfect CNTs indicates that some vibrational states arising from the defects emerge in the silent vibrational regions of the perfect ones (shown in Fig. 3). Further analysis finds that two types of typical modes appear in each VDOS of the defective tubes, and the common characters of the patterns are that the amplitudes of displacements of the atoms subject to the single vacancy are much larger than those of the atoms being far away from the defect, which strongly indicates that both mode A and mode B (marked in Fig. 3) are induced by the single vacancy. Evidently, the frequencies of the mode A are 1028.6, 1036.5 and 1019.5 cm^{-1}, and the frequencies of the mode B are 1170.1, 1168.1 and 1163.8 cm^{-1}, for tubes of (n, 0) with n=7−9, respectively. The frequencies of modes A and B vary slightly with the changes of the radii of the tubes, which indicate that they are insensitive to the size of the tube. As a representative, the local vibrational patterns of mode A and mode B for (7, 0) tube are displayed in Fig. 4. In mode A [shown in Fig. 4 (a)], two atoms of both C1 and C2, the nearest atoms to the DB atom in the pentagon, are subject to the largest amplitude of their displacements, whereas C3 has a slight displacement. For mode B as shown in Fig. 4 (b), C1, C2 and the DB atom deviate from their equilibrium positions to the void or deviate in a reverse direction. Meanwhile, C3 and two neighboring atoms of the DB atom make a certain contribution to this mode. Similar results are obtained from calculations at the level of the

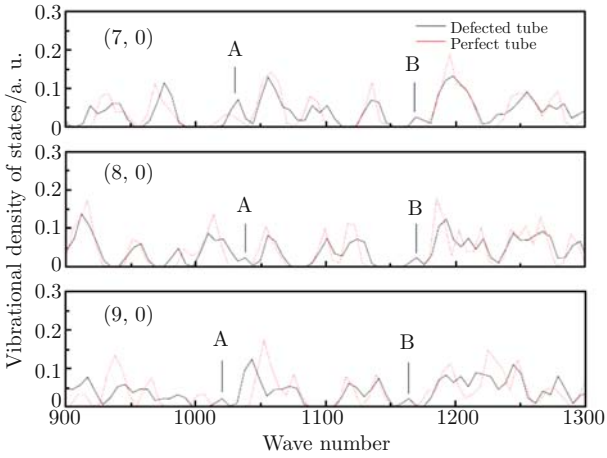

Fig. 3 VDOS of the concerned defective tubes and their related perfect tubes. The modes marked A and B indicate two concerned modes. Reprinted with permission from Ref. [36].

Perdew–Burke–Ernzerhof generalized gradient approximation (GGA–PBE) [41]. Therefore, these two types of modes can be regarded as the fingerprint of a 5-1DB defect in a CNT. Moreover, calculations using the empirical bond polarizability model [42, 43] predict that both mode A and mode B are Raman active. For (7, 0) tube, the intensities of the Raman modes in the frequency range of 900−1300 cm^{-1} are displayed in Fig. 5, in which the intensities of both mode A and mode B are observed to be much stronger than the others. This shows that the single vacancies in CNTs can probably be probed via detecting the signals of mode A and mode B in Raman spectra.

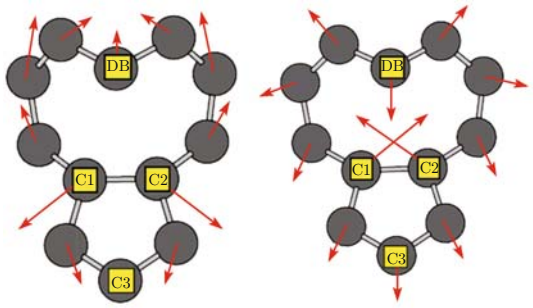

Fig. 4 The local vibrational features near the 5-1DB defect in a (7, 0) tube for **(a)** mode A and **(b)** mode B. The relevant atoms are labeled. Reprinted with permission from Ref. [36].

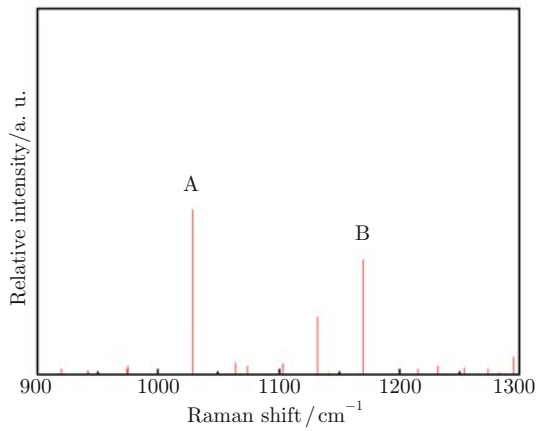

Fig. 5 The relative Raman intensity of mode A and mode B for (7, 0) carbon nanotube. Reprinted with permission from Ref. [36].

2.3 Interaction between a single vacancy and adsorbates

The interaction between the CNTs and adsorbates has been studied extensively [14, 44–49]. To date, various adsorbates, such as many kinds of molecules, radicals, and some metals have been taken into account, among which the hydrogen adsorption has been paid much attention to. This is because carbon nanotubes are desired to be hydrogen storage cells. The studies reveal that hydrogen molecules favorably physisorb at the exterior surface of a CNT or in the interstitial region between carbon nanotubes at room temperature and under hydrogen pressure of about 1 atm [50–55]. In contrast, when the air pressure around the carbon nanotubes increases, the H–H bond of a hydrogen molecule is broken, and the dissociated hydrogen atoms chemisorb on the outer wall of a CNT [45]. In addition to the outer wall, hydrogen adsorbing on the interior surface of a carbon nanotube can also take place. It is pointed out that the former case is preferential, due to the curvature effect of the cylindrical structures of the tubes [44].

When a single vacancy presents in a CNT, it prefers to capture hydrogen nearby. Based on the tight binding approximation, the interaction of either a hydrogen atom or a hydrogen molecule with a (12, 0) tube containing a single vacancy has been studied [56]. It is found that a hydrogen atom should overcome an energy barrier of 0.94 eV to adsorb on the perfect wall of the tube, which is essentially ascribed to the hybridization of the adsorbed site transformed from sp^2 to sp^3. In contrast, a hydrogen atom can adsorb on the dangling bond site of a 5-1DB defect without any energy cost. For a hydrogen atom adsorbing on the DB site, there are a lowest energy configuration and two metastable configurations. The energy difference between these configurations is less than 1.1 eV, so one can speculate that the adsorbed hydrogen can transform between these low-energy sites at room temperature.

For a hydrogen molecule, it can adsorb on the perfect region of the tube by undergoing an energy barrier of 2.9 eV, while on the DB site by overcoming an energy barrier of no more than 1.6 eV. These energy barriers are much higher than those for a hydrogen atom respectively adsorbing on the perfect wall and the DB site of the CNT. For adsorption of a hydrogen molecule on the DB atom, there are two kinds of final configurations: the adsorbed hydrogen molecule is either dissociated or not dissociated, corresponding to sp^3-like or sp^2-like hybridization, and the former is more stable.

The results above imply that existence of a 5-1DB defect facilitates the adsorption of either a hydrogen atom or a hydrogen molecule on the defective tube effectively. Because hydrogen storage is an important application of CNTs, an interesting question is whether such an interaction between the defect and hydrogen influences the gas storage capacity or not. A previous work has reported that the existence of microvoids in CNTs enhances the hydrogen adsorption on the tube walls, but reduces the gas storage capabilities of the tubes [49]. In fact, it can be inferred that the gas leakage of a CNT is somewhat dependent on the sizes of the microvoids in the tubes. It is revealed that adsorption of a single hydrogen molecule on the DB site from the inner wall of (12, 0) tube is fairly difficult, which is due to that a very high energy barrier of about 2.9 eV hinders the adsorption of hydrogen. This

indicates that adsorption of a hydrogen molecule on the DB site rarely occurs on the interior surface of the carbon nanotube. On the other hand, flipping a single hydrogen atom attached at the DB atom into the inner area of (12, 0) tube costs energy of more than 3.1 eV, which means that the flip-in mechanism for a single hydrogen atom through the 5-1DB defect is almost impossible. Similarly, kicking a dissociated hydrogen molecule adsorbed on the DB atom into the CNT is also hindered by the high energy barrier of 3.5 eV. Therefore, both flip-in and kick-in mechanism for hydrogen entering the inner region through the single vacancy in a carbon nanotube are ruled out at least at room temperature and normal atmospheric pressure.

However, it is noted that if we replace a single vacancy by a divacancy in (12, 0) tube, either a single hydrogen atom or a single hydrogen molecule can probably traverse between the outer and inner sides via the divacancy. As a result, it is strongly suggested that hydrogen leakage and hydrogen fill-in for the defective carbon nanotubes containing divacancies or defects supplying larger-sized voids should be taken into account when the tubes serve as storage cells for hydrogen molecules.

In addition to hydrogen, small hydrocarbon radicals (–CH, $–CH_2$, $–CH_3$) interacting with single vacancies in CNTs have been studied systematically [57–59]. Each of these radicals can adsorb on the single vacancies in the concerned (n, 0) (n=9−12) carbon nanotubes without any energy cost. More interestingly, it is found that the adsorbed –CH or $–CH_2$ at the DB site of a 5-1DB defect can convert the local structure of the 5-1DB defect to be the perfect network at low temperatures [57]. As shown in Fig. 6 (a), when the system is heated to 100 K, the adsorbed –CH first connects with two carbon atoms (C1 and C2) in the pentagon, then breaks the C1-C2 bond in the pentagon. Consequently, the adsorbed –CH converts the local structure to be a hexagonal network with attachment of a hydrogen atom [Fig. 6 (b)]. This attached hydrogen escapes at 600 K, and the local structure of the defect is healed completely. Similarly, the adsorbed $–CH_2$ at DB site breaks the corresponding C1-C2 bond in the pentagon, and the carbon atom in the radical rebonds to C1 and C2 at 300 K, converting the structure of the 5-1DB defect to be a perfect network with attachment of two hydrogen atoms [Fig. 6(c)]. Such a configuration is unfavorable, thus one of the hydrogen atoms flees at 300 K. When the temperature reaches 600 K, the second hydrogen atom gets away. However, the attached radical $–CH_3$ does not improve the local structure of the 5-1DB defect anyway, even if the temperature of the system reaches 600 K.

These adsorbed radicals at the DB sites exhibit different abilities of improving the local structures of the single vacancies, which is essentially ascribed to the different reactivity of the radicals. For example, a –CH, $–CH_2$ or $–CH_3$ bonding with a DB carbon atom in a CNT just removes two dangling bonds of the system. For the adsorbed –CH and $–CH_2$, they still respectively remain two and one dangling bond(s), having possibilities to bond with the carbon atoms nearby. In contrast, the adsorbed $–CH_3$ is just saturated by the DB atom of the 5-1DB defect, forming a stable configuration. So, the adsorbed –CH and $–CH_2$ improve the structure of the 5-1DB defect in a CNT, while $–CH_3$ does not. In addition, it is noted that the temperature effect is a critical factor to improve the structure of the single vacancies. Driven by the temperature effect, the C–C bonds near the 5-1DB defect are considerably enlarged, and become weak significantly, which assists the structural transformation of the 5-1DB defect.

In addition to the single vacancies, the defect free region of the outer wall of a CNT is also a good place for small hydrocarbon radicals to adsorb [58]. The favorable adsorption sites for –CH and $–CH_2$ are the bond centers of C–C bonds parallel to the axis of the tubes, and that for $–CH_3$ is atop sites of the carbon atoms. For a typical (9, 0) tube, the adsorption energy barriers for –CH and $–CH_2$ are less than 0.4 eV, and that for $–CH_3$ is about 0.89 eV. Moreover, the diffusion behaviors of these radicals on the outer wall of the CNT are predicted [58]to be that: both –CH and $–CH_2$ prefer to zigzag on the outer wall, by passing through alternately two kinds of C–C bonds which are either parallel or perpendicular to the tube axis. Differently, the $–CH_3$ radical prefers to hop from atop of a carbon atom to another via the related bond center. For –CH and $–CH_2$, the highest energy bar-

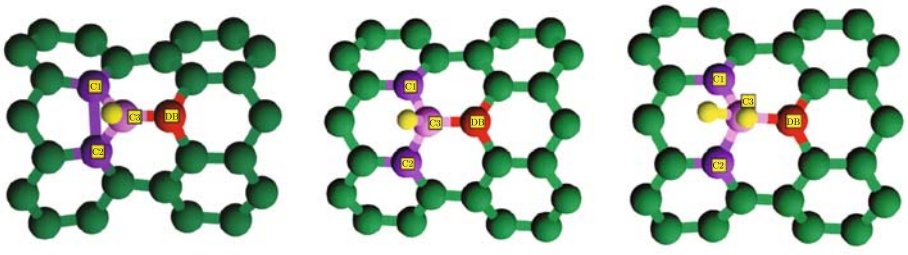

(a) (b) (c)

Fig. 6 Snapshots for the structural transformation of a monovacancy induced by: **(a), (b)** –CH and **(c)** $–CH_2$ respectively adsorbing on the DB atom in the (9, 0) CNT. Reprinted with permission from Ref. [57].

riers are less than 1.3 eV, corresponding to the antibond sites of the tilted C–C bonds. For $-CH_3$, the diffusion barriers are less than 1.1 eV, which are just at the bond centers of C–C bonds. According to the previous reports [60,61], the diffusion barriers of less than 1.3 eV mean that the radicals of –CH, $-CH_2$ and $-CH_3$ have possibilities to diffuse on the outer wall of the tube at room temperature.

Since the radicals can adsorb and diffuse in the perfect region of a CNT, it is possible for them to approach to a 5-1DB defect in the tube. To find the diffusion behaviors of the radicals near a 5-1DB defect, the potential energy surface for each radical migrating in a large region containing a 5-1DB defect in (9, 0) tube is calculated, in which the typical sites near the defect are labeled with characters, as shown in Fig. 7. The calculated potential energy surfaces for the cases of –CH, $-CH_2$ and $-CH_3$ are shown in Fig. 8(a)−(c), where the minimum energy of each radical on the perfect tube is taken as a reference for the related case. It shows clearly that an obvious wide lower-energy region appears around the 5-1DB defect, and three typical low-energy paths exists in each of the potential energy surfaces, of which two symmetric striped patterns are identified to be the edges of the pentagon, and the third one is around the DB atom. Moreover, each of the potential energy surfaces shows that the energy of each system drops dramatically when a radical locates near the void of the 5-1DB defect, especially for the adsorption of –CH. The nearer the radical approaches to the void of the 5-1DB, the more energy of the system drops, which indicates that the 5-1DB defect is just like a trap which can capture a migrating radical nearby.

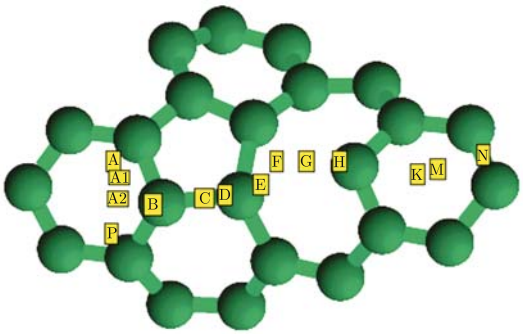

Fig. 7 The local atomic structure near the 5-1DB defect. Some typical sites are labeled with characters. Reprinted with permission from Ref. [58].

A typical diffusion pathway for –CH is from the defect free region (N site) to the DB site (H) of the 5-1DB defect via M and K sites. The calculated diffusion barriers are less than 0.6 eV. Furthermore, once –CH adsorbs on DB site, it can reach the F site in the void of the 5-1DB by overcoming a lower energy barrier (about 0.50 eV). At the F site, the 5-1DB defect surprisingly converts to be the perfect network. Another typical diffusion pathway for –CH is to the pentagon. At the edge of the pentagon (site B), –CH breaks the bond of a C–C in the pentagon, and the local structure is rearranged to be an overturned 5-1DB defect with attaching of –CH at the DB atom in this defect. This situation is somewhat equivalent to the adsorption of –CH at H site, so –CH at B site can further heal the defect with a low energy cost as it does at H site.

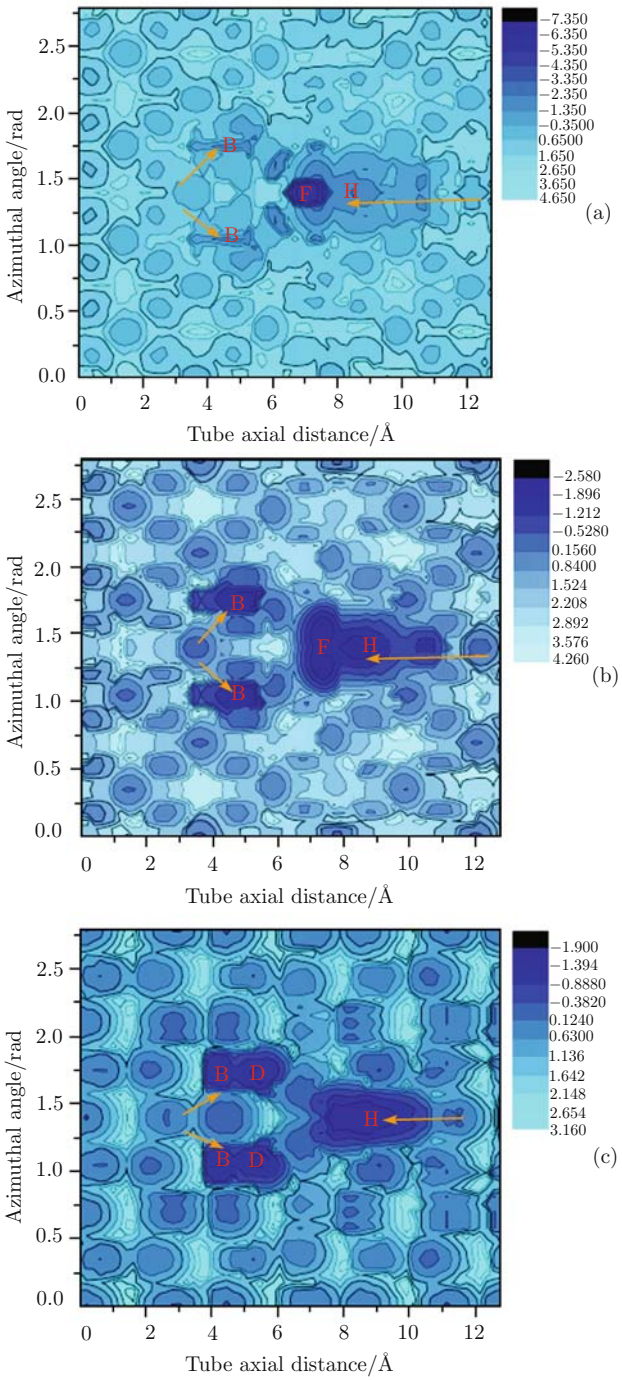

Fig. 8 The potential energy surface for **(a)** –CH, **(b)** $-CH_2$ and **(c)** $-CH_3$ adsorbed at the sites in the selected region. The typical pathways for each radical migrating from the defect-free region to the 5-1DB defect are guided with solid-line arrows. The typical sites labeled with the character of H, F, D or B refers to Fig. 7, and another character of B and D are labeled in view of symmetry. Reprinted with permission from Ref. [58].

The diffusion pathways for $-CH_2$ are almost the same as those of –CH, except for F site. At this site, $-CH_2$ does not heal the 5-1DB defect, but improves the local structure by bridging the pentagon and the DB atom. For $-CH_3$, the lowest energy site of its adsorption is the DB site. Similar to –CH and $-CH_2$, $-CH_3$ overturns the 5-1DB defect at site B, with attachment of the $-CH_3$ radical on the new DB atom. As a result, both –CH and $-CH_2$ can improve the structure of the 5-1DB defect effectively by diffusing to either the pentagon or the DB atom, whereas $-CH_3$ does not improve the structure of the 5-1DB defect anyway.

An adsorbed radical either in the defect free region or on a single vacancy in a CNT influences the electronic structure of the tube. The density of states for a perfect (7, 0) tube with adsorption of each considered radical is shown in Fig. 9(a)−(c). Obviously, the adsorbed radicals alter the electronic structure of the tube, especially near the band edges, where the majority spin states (*upper curves*) and the minority spin states (*lower curves*) are plotted separately. For the adsorption of either –CH or $-CH_2$, the induced defect states appear near the edges of the valence band and conduction band; For the $-CH_3$ adsorption, two peaks in DOS are observed at –0.1 eV (majority spin state) and +0.1 eV (minority spin state) with respect to the Fermi level (E_F). The calculated local density of states (LDOS) reveals that the edge states in the cases of –CH and $-CH_2$ mainly come from the contribution of the carbon atoms near the adsorption site. With adsorption of either –CH or $-CH_2$, the carbon atoms in the CNT that bond with the radical undergo the transition from sp^2 to sp^3 hybridization, with occurrence of longer bonds (1.50 Å) and shorter bonds of (1.40 A) around the adsorption site. These strained bonds cause the edge states near the band gap. In contrast, the adsorbed $-CH_3$ pulls the bonded carbon atom in CNT out of the tube wall significantly. This not only induces weak bonds (about 1.53 Å) around the bonded carbon atom, but also causes unpaired electron(s) in the neighboring carbon atoms. As a result, these unpaired electron(s) contributed to the local states near the Fermi level.

In the case of a radical adsorbing on the DB atom, the DB atom together with its nearest neighboring carbon atoms, is rearranged to form a local planar configuration, with strained C–C bonds. These strained bonds together with the carbon atoms in the pentagon and the octagon give rise to the defect states, narrowing the gap width of the tube significantly [Fig. 9(d)−(f)]. In addition, a sharp peak at about –0.6 eV (marked with A) presents in each calculated DOS. These peaks are originated from the carbon atoms in the pentagon. Furthermore, it is found that these defect states near the band gap are not from the adsorbed radicals directly, but from

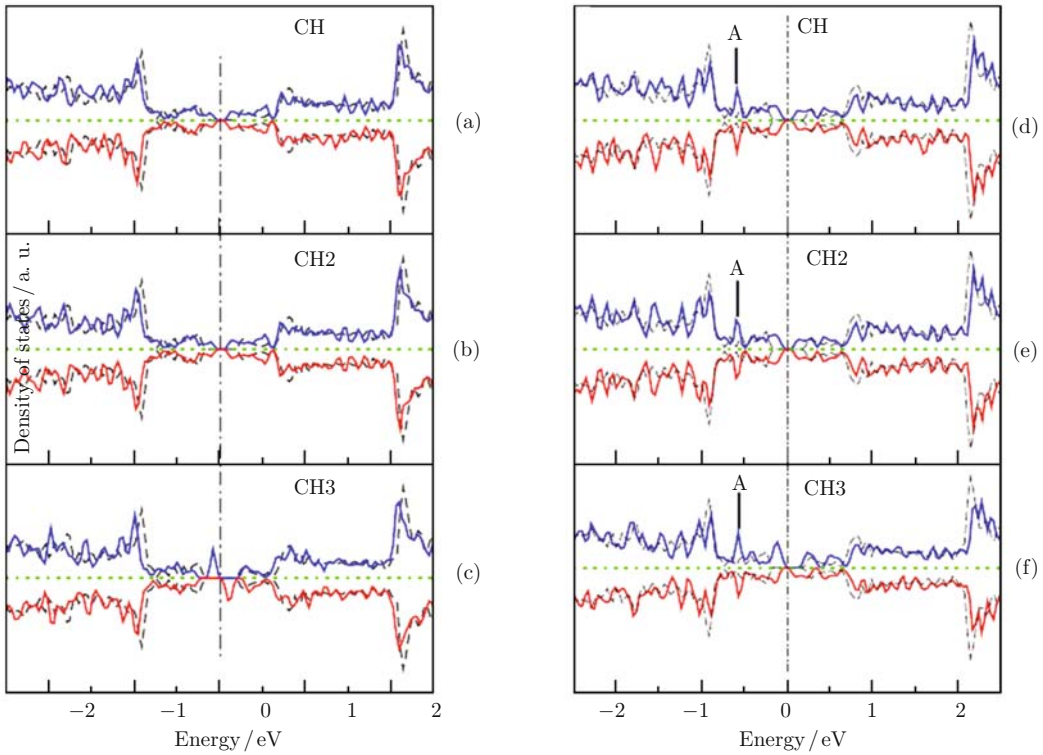

Fig. 9 The total electronic density of states for **(a)** –CH, **(b)** $-CH_2$ and **(c)** $-CH_3$ adsorbed in perfect network of (7, 0) tube, as well as the total electronic density of states for **(d)** –CH, **(e)** $-CH_2$ and **(f)** $-CH_3$ adsorbed at the dangling bond of a 5-1DB defect in (7,0) tube. The majority spin states and the minority spin states are shown with blue and red solid lines, upper and lower, respectively. The black dashed lines in **(a)**, **(b)** and **(c)** stand for the total density of states of the perfect (7, 0) tube. The dot-dash lines indicate the Fermi levels, which are shifted to zero. Reprinted with permission from Ref. [59].

the distorted structures near the adsorption sites.

3 Stone–Wales (SW) defects

An SW defect can be created by rotating one of the C–C bonds by $\pi/2$ from its initial site, forming two heptagons and two pentagons in local structure. Therefore, it is also called as 5–77–5 defect. Up to now, the formation mechanism of the SW defect in a carbon nanotube is unclear. There are several possible ways to form an SW defect. Rotating one of the C–C bonds to form an SW defect is termed as direct exchange of the C–C bond. In this way, the lowest-energy barrier for the bond rotation in a tube governs the possibility of the formation process of an SW defect. A previous tight-binding calculation [62] has predicted a lowest-energy barrier of 4.0 eV for bond rotation in a (6, 6) tube. Therefore, the activated energy, which is defined as the sum of the formation energy and the migration energy barrier, of the SW defect created with the direct-exchange method in a (6, 6) tube is as high as 6.0 eV [25]. Combining this value with the temperature of about 4000 K in the center of the arc discharge [63], it can be believed that there is little chance to generate an SW defect in a (6, 6) CNT by directly rotating a C–C bond driven by an arc discharge. Nevertheless, the direct-exchange mechanism is also not suitable for explaining the formation of an SW defect on most carbon nanotubes. On the other hand, it is found that an SW defect can be easily induced by an axial strain imposed on an armchair tube, because the formation of the SW defect may release the strain in the tube [30, 91]. In addition, SW defects frequently appear at the cores relevant to structural transformations, such as the coalescence of nanotubes [64] and the formation of pure intramolecular junctions of nanoelectronic devices [19, 65]. Also, there is a good possibility of formation of SW defects at the end of a CNT during growth [29].

Once the SW defects are present in a carbon nanotube, they can significantly change the conductance of the tube [66, 67]. Two remarkable dips in the conductance curve, which lie above by 0.53 eV and below by –1.03 eV with respect to the Fermi energy of the CNTs respectively, are induced by the defect. This indicates that there are some quasibound states induced by the presence of the SW defect.

For either $(n, 0)$ or (n, n) CNTs, the C–C bonds can be sorted as two groups according to their inequivalent orientations. Therefore, there are two kinds of features for SW defects in each kind of CNT, which are grouped into $(n, 0)$-I, $(n, 0)$-II, (n, n)-I and (n, n)-II as shown in Fig. 10. The formation energies of these defects with different orientations are found to be different [25]. Meanwhile, the smaller the size of a tube with the SW defect is, the lower the formation energy of the system is, which indicates that an SW defect preferentially occurs in the small-sized carbon nanotubes. Moreover, for the tubes with the same radius, the order of the defect formation energy is $E(n, n)$-I$>E(n, 0)$-II$>E(n, n)$-II$>E(n, 0)$-I. This implies that the $(n, 0)$-I defect is the most favorable energetically to occur in the $(n, 0)$ tubes. In addition, the formation energy curve for $(n, 0)$-I is quite close to that of (n, n)-II.

On the other hand, the relation between the formation energy of the SW defect in a CNT and the radius of the CNT is also investigated. It is revealed that the formation energies of the SW defects in the tubes of (7, 0),

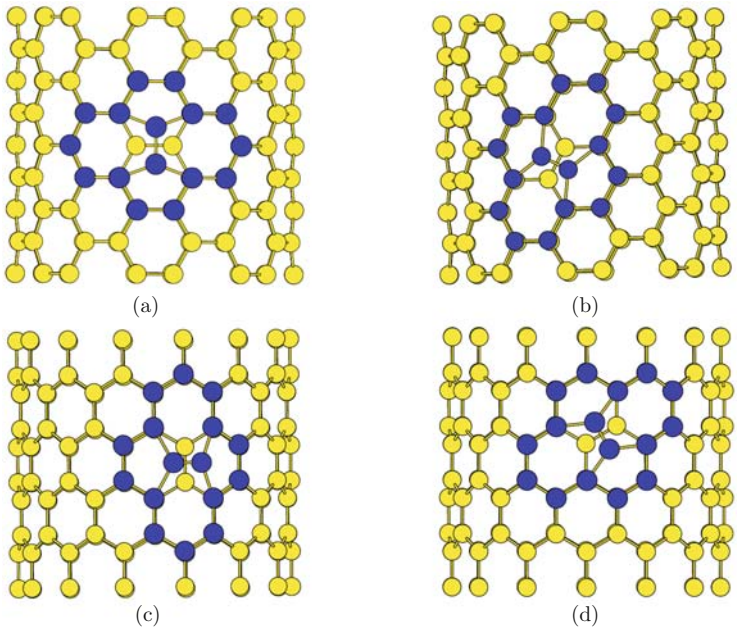

Fig. 10 The structural patterns for a Stone–Wales defect of **(a)** (n, n)-I, **(b)** (n, n)-II, **(c)** $(n, 0)$-I and **(d)** $(n, 0)$-II.

(6, 2), (5, 3) and (4, 4), which had almost equal radius and different chiral angles, decrease as the chiral angles of the tubes increase. Therefore, the formation energy of the SW defect in a tube is strikingly dependent on the chirality of the tube.

In addition, many efforts have been made to identify such common topologic defects in CNTs via observed spectroscopy. By combining resonant photoabsorption and vibration spectroscopy with scanning tunneling microscopy and time dependent density functional calculations, Miyamoto [68] unambiguously identified the SW defects in carbon nanotubes. It is suggested that the vibrational mode with the frequency of 1962 cm^{-1} associated with the SW defect can serve as a fingerprint for such a defect in a CNT. Moreover, some distinct features in the bias-dependent STM images are also regarded as an indicator of SW defects existing in CNTs.

4 Summary

In this paper, we review the progress of research in the structural defects in carbon nanotubes, of which single vacancies and stone-wales defects are mainly focused on. In a carbon nanotube, the structural transition from an ideal single vacancy to a 5-1DB defect, together with the related electronic and vibrational properties is reviewed in detail. Moreover, the interaction of the single vacancy with hydrogen and hydrocarbon radicals is addressed. In addition, the stability of Stone–Wales defects in carbon nanotubes with different sizes and different chirality is also discussed. The stability of an SW defect in CNT is strongly dependent on the size and chirality of the tube.

Acknowledgements This work was financially supported by the National Basic Research Program of China (Grant Nos. 2006CB922000 and 2009CB939901), the National Natural Science Foundation of China (Grant Nos. 50121202 and 60444005), and the USTC-HP HPC project. The authors thank A. J. Lu, W. S. Yang and R. L. Zhou for their contributions to this review article.

References

1. S. Iijima, Nature (London), 1991, 354: 56
2. H. Dai, J. H. Hafner, A. G. Rinzler, D. T. Ccbert, and R. E. Smalley, Nature(London), 1996, 384: 147
3. P. Kim and C. M. Lieber, Science, 1999, 286: 2148
4. P. Pancharal, Z. L. Wang, D. Ugarte, and W. de Heer, Science, 1999, 283: 1513
5. S. J. Tans, R. M. Verschueren, and C. Dekker, Nature (London), 1999, 393: 49
6. R. S. Friedman, N. C. McAlpine, D. S. Ricketts, D. Ham, and C. M. Lieber, Nature (London), 2005, 434: 1085
7. M. S. Dresselhaus and P. C. Eklund, Adv. Phys., 2000, 49: 705
8. A. M. Rao, E. Richter, S. Bandow, B. Chase, P. C. Eklund, K. W. Williams, M. Menon, K. R. Subbaswamy, A. Thess, R. E. Smalley, G. Dresselhaus, and M. S. Dresselhaus, Science, 1997, 275: 187
9. A. Kasuya, Y. Sasaki, Y. Saito, K. Tohji, and Y. Nishina, Phys. Rev. Lett., 1997, 78: 4434
10. J. Hone, B. Batlogg, Z. Benes, A. T. Johnson, and J. E. Fischer, Science, 2000, 289: 1730
11. R. A. Jishi, L. Venkataraman, M. S. Dresselhaus, and G. Dresselhaus, Chem. Phys. Lett., 1993, 209: 77
12. D. B. Mawhinney, V. Naumenko, A. Kuznetsova, J. T. Yates, Jr. J. Liu, and R. E. Smalley, Chem. Phys. Lett., 2000, 324: 213
13. M. Volpe and F. Cleri, Chem. Phys. Lett., 2003, 371: 476
14. O. Gulseren, T. Yildirim, and S. Ciraci, Phys. Rev. B, 2002, 66: 121401
15. J. C. Charlier, T. W. Ebbesen, and Ph. Lambin, Phys. Rev. B, 1996, 53: 11108
16. P. M. Ajayan, V. Ravikumar, and J. C. Charlier, Phys. Rev. Lett., 1998, 81: 1437
17. A. J. Lu and B. C. Pan, Phys. Rev. Lett., 2004, 92: 105504
18. A. V. Krasheninnikov, K. Nordlund, M. Sirvio, E. Salonen, and J. Keinonen, Phys. Rev. B, 2001, 63: 245405
19. V. H. Crespi, M. L. Cohen, and A. Rubio, Phys. Rev. Lett., 1997, 79: 2093
20. V. H. Crespi, N. G. Chopra, M. L. Cohen, A. Zettle, and S. G. Louie, Phys. Rev. B, 1996, 54: 5927
21. A. Hansson, M. Paulsson, and S. Stafstrom, Phys. Rev. B, 2000, 62: 7639
22. Y. F. Zhu, T. Yi, B. Zheng, and L. L. Cao, Appl. Surf. Sci., 1999, 137: 83
23. M. Terrones, H. Terrones, F. Banhart, J. C. Charlier, and P. M. Ajayan, Science, 2000, 288: 1226
24. J. Rossato, R. J. Baierle, A. Fazzio, and R. Mota, Nano Lett., 2005, 5: 197
25. B. C. Pan, W. S. Yang, and J. L. Yang, Phys. Rev. B, 2000, 62: 12652
26. S. Lee, G. Kim, H. Kim, B. Y. Choi, J. Lee, B. W. Jeong, J. Ihm, Y. Kuk, and S. J. Kahng, Phys. Rev. Lett., 2005, 95: 166402
27. S. L. Zhang, S. L. Mielke, R. Khare, D. Troya, R. S. Ruoff, G. C. Schatz, and T. Belytschko, Phys. Rev. B, 2005, 71: 115403
28. J. Han, M. P. Anantram, R. L. Jaffe, J. Kong, and H. Dai, Phys. Rev. B, 1998, 57: 14983
29. D. L. Carroll, P. Redlich, P. M. Ajayan, J. C. Charlier, X. Blase, A. De vita, and R. Car, Phys. Rev. Lett., 1997, 78: 2811
30. M. B. Nardelli, B. I. Yakobson, and J. Bernholc, Phys. Rev. B, 1998, 57: R4277
31. M. B. Nardelli, B. I. Yakobson, and J. Bernholc, Phys. Rev. Lett., 1998, 81: 4656
32. V. H. Crespi, M. L. Cohen, and A. Rubio, Phys. Rev. Lett., 1997, 79: 2093
33. L. Chico, L. X. Benedict, S. G. Louie, and M. L. Cohen, Phys. Rev. B, 1996, 54: 2600
34. A. Rubio, Appl. Phys. A: Mater. Sci. Process, 1999, 68: 275
35. L. G. Bulusheva, A. V. Okotrub, and D. A. Romanov, J. Phys. Chem. A, 1998, 102: 975
36. H. Y. He, and B. C. Pan, Phys. Rev. B, 2008, 77: 073410

37. D. Sanchez-Portal, P. Ordejon, E. Artacho, and J. M. Soler, Int. J. Quantum Chem., 1997, 65: 453
38. N. Troullier and J. L. Martins, Phys. Rev. B, 1991, 43: 1993
39. J. M. Soler, E. Artacho, J. D. Gale, A. Garcia, J. Junquera, P. Ordejon, and D. Sanchez-Portal, J. Phys.: Condens. Matter, 2002, 14: 2745, and references therein
40. M. T. Yin and M. L. Cohen, Phys. Rev. B, 1982, 26: 3259
41. J. P. Perdew, K. Burke, and M. Ernzerhof, Phys. Rev. Lett., 1996, 77: 3865
42. S. Guha, J. Menendez, J. B. Page, and G. B. Adams, Phys. Rev. B, 1996, 53: 13106
43. R. Saito, T. Takeya, T. Kimura, G. Dresselhaus, and M. S. Dresselhaus, Phys. Rev. B, 1998, 57: 4145
44. K. Tada, S. Furuya, and K. Watanabe, Phys. Rev. B, 2001, 63: 155405
45. T. Yildirim, O. Gulseren, and S. Ciraci, Phys. Rev. B, 2001, 64: 075404
46. S. M. Lee, K. Hyeok, Y. H. Lee, G. Seifert, and T. Frauenheim, J. Am. Chem. Soc., 2001, 123: 5059
47. J. S. Arellano, L. M. Molina, A. Rubio, M. J. Lopez, and J. A. Alonso, J. Chem. Phys., 2002, 117: 2281
48. S. P. Chan, G. Chen, X. G. Gong, and Z. F. Liu, Phys. Rev. Lett., 2001, 87: 205502
49. M. Volpe and F. Cleri, Chem. Phys. Lett., 2003, 371: 476
50. K. A. Williams and P. C. Eklund, Chem. Phys. Lett., 2000, 320: 352
51. M. Shiraishi, T. Takenobu, and M. Ata, Chem. Phys. Lett., 2003, 367: 633
52. J. J. Zhao, A. Buldum, J. Han, and J. P. Lu, Nanotechnology, 2002, 13: 195
53. Y. C. Ma, Y. Y. Xia, M. W. Zhao, and N. M. Ying, Chem. Phys. Lett., 2002, 357: 97
54. V. V. Simonyan, P. Diep, and J. K. Johnson, J. Chem. Phys., 1999, 111: 9778
55. M. Boustimi, J. Baudon, P. Candori, and J. Robert, Phys. Rev. B, 2002, 65: 155402
56. A. J. Lu and B. C. Pan, Phys. Rev. B, 2005, 71: 165416
57. R. L. Zhou, H. Y. He, and B. C. Pan, Phys. Rev. B, 2007, 75: 113401
58. H. Y. He and B. C. Pan, Physica E, 2008, 40: 542
59. H. Y. He and B. C. Pan, J. Phys. Chem. C, 2008, 112: 18876
60. T. Sato, S. Kitamura, and M. Iwatsuki, J. Vac. Sci. Technol. A, 2000, 18: 960
61. H. M. Branz and S. B. Zhang, Mat. Res. Soc. Symp., 2001, 664: A13.3.1
62. P. H. Zhang, P. E. Lammert, and V. H. Crespi, Phys. Rev. Lett., 1998, 81: 5346
63. V. H. Crespi, Phys. Rev. Lett., 1999, 82: 2908
64. M. Yoon, S. Han, G. Kim, S. Lee, S. Berber, E. Zosawa, J. Ihm, M. Terrones, F. Banhart, J. C. Charlier, N. Grobert, H. Terrones, P. M. Ajayan, and D. Tomanek, Phys. Rev. Lett., 2004, 92: 075504
65. M. Ouyang, J. L. Huang, C. L. Cheung, and C. M. Lieber, Science, 2001, 291: 97
66. H. J. Choi, J. Ihm, S. G. Louie, M. L. Cohen, Phys. Rev. Lett., 2000, 84: 2917
67. H. T. Yang, L. F. Yang, J. W. Chen, and J. M. Dong, Phys. Lett. A, 2004, 325: 287
68. Y. Miyamoto, A. Rubio, S. Berber, M. Yoon, and D. Tomanek, Phys. Rev. B, 2004, 69: 121413(R)